Inorg. Chem. **2007**, *46*, 3313–3321

Photochromism of Novel Metal Coordination Polymers with 1,2-Bis(2′-methyl-5′-(carboxylic acid)-3′-thienyl)perfluorocyclopentene in the Crystalline Phase

Jing Han,[†] Masahiko Maekawa,[‡] Yusaku Suenaga,[†] Hideaki Ebisu,[†] Atsuhiro Nabei,[†] Takayoshi Kuroda-Sowa,[†] and Megumu Munakata*,[†]

Department of Chemistry, Kinki University, Kowakae, Higashi-Osaka, Osaka, Research Institute for Science and Technology, Kinki University, Kowakae, Higashi-Osaka, Osaka 577-8502, Japan

Received August 11, 2006

Three new metal complexes with 1,2-bis(2′-methyl-5′-(carboxylic acid)-3′-thienyl)perfluorocyclopentene (BM-5-CATP) were synthesized and characterized by X-ray diffraction analysis. BM-5-CATP serves as a bis-monodentate ligand that bridges metal centers to generate three 1D polymers. The two thienyl rings in the three complexes adopt antiparallel fashions, and the distances of 3.39, 3.53, and 3.57 Å between the two reactive carbons are short enough to allow photocyclizations to occur in the crystalline phase. $[Co(BM\text{-}5\text{-}CATP)(py)_2(MeOH)_2]$ (**1**) displayed effective photoisomerization in the crystalline phase. Interestingly, solvated **1** underwent a solid-state conversion upon heating to generate, through the release of the coordinated MeOH and rearrangement of the coordination geometry, the desolvated form (**1a**), while maintaining reversible photochromism. The removal of the solvent led to obvious changes in physical properties such as color and magnetic properties. The ESR spectra of **1** and **1a** changed reversibly upon photoexcitation, indicating changes in coordination geometry accompanied by photoreaction. The magnetic susceptibilities of **1** and **1a** showed no obvious changes, suggesting that the cobalt–cobalt interaction through the long bridging BM-5-CATP is less effective. Both $[Cu(BM\text{-}5\text{-}CATP)(py)_3](EtOH)(py)_{1.8}$ (**2**) and $[Zn(BM\text{-}5\text{-}CATP)(phen)(H_2O)]$ (**3**) exhibited reversible photoreactions in the crystalline phase. However, **3** did not show remarkable spectral changes because of steric hindrance from the coordinated bulky phenanthroline and the intramolecular H bonds.

Introduction

Crystal engineering of metal−organic frameworks (MOFs) has attracted much attention thanks to the generation in recent decades of materials with interesting topologies and technologically useful functions. Through rational design and precise control of the properties of building blocks such as shape, symmetry, flexibility, functionality, and synthesized conditions, a remarkable class of materials containing diverse architectures and many functions could be obtained; although, the prediction of the resulting structures still remains a great challenge. One of the important targets in recent research is to produce a hybrid system having multifunctionality coupled with transport, optical, and magnetic properties.[1]

Considerable efforts have been dedicated to photochromic compounds because of their potential to be used for optical memory media, photonic switch devices, and photodrive actuators. Among the known photochromic systems, diarylethene bearing two thienyl-derived groups (bisthienylethene) is cited as the best candidate, owing to its outstanding thermal stability, excellent photofatigue resistance, high sensitivity, and characteristic bistability.[2] It inherently exhibits two different chemical forms (open and closed), which are reversibly interconverted in response to optical stimulation. The open-ring and closed-ring isomers differ from each other

* To whom correspondence should be addressed. E-mail: munakata@chem.kindai.ac.jp. Tel: +81-6-6721-2332-(4119). Fax: +81-6-6721-2721.
[†] Department of Chemistry.
[‡] Research Institute for Science and Technology.

(1) (a) Coronado, E.; Galán-Mascaró, J. R.; Gómez-García, C. J.; Laukhin, V. *Nature* **2000**, *408*, 447−449. (b) Uji, S.; Shinagawa, H.; Terashima, T.; Yakabe, T.; Terai, Y.; Tokumoto, M.; Kobayashi, A.; Tanaka, H.; Kobayashi, H. *Nature* **2001**, *410*, 908−909. (c) Okubo, M.; Enomoto, M.; Koyama, K.; Uwatoko, Y.; Kojima, N. *Bull. Chem. Soc. Jpn.* **2005**, *78*, 1054−1060. (d) Itoi, M.; Ono, Y.; Kojima, N.; Kato, K.; Osaka, K.; Takata, M. *Eur. J. Inorg. Chem.* **2006**, *45*, 1198−1207.

(2) (a) Gilat, S. L.; Kawasi, S. H.; Lehn, J.-M. *Chem.—Eur. J.* **1995**, *1*, 275−284. (b) Kawasi, S. H.; Gilat, S. L.; Ponsinet, R. *Chem.—Eur. J.* **1995**, *1*, 285−293. (c) Yamada, T.; Kobatake, S.; Muto, K.; Irie, M. *J. Am. Chem. Soc.* **2000**, *122*, 1589−1592. (d) Higashiguchi, K.; Matsuda, K.; Irie, M. *Angew. Chem., Int. Ed.* **2003**, *42*, 3537−3540.

10.1021/ic0615168 CCC: $37.00
Published on Web 03/22/2007

not only in absorption spectra but also in various physical and chemical properties such as geometrical structure, optical rotation, refractive index, dielectric constant, and fluorescence.[3] It is noted that bisthienylethene could undergo photochromism effectively, not only in solution but also in the single-crystalline phase.[4] In crystals, the photocyclization quantum yield is 2 times larger than that in solution, whereas the activation energy of the cycloreversion reaction is smaller than that in solution.[5] Furthermore, when metal ions are located at both of the terminal positions of the thienyl groups of bisthienylethene, the interaction between the metal ions can be switched by photoirradiation because the π-conjugated bond structures between the two thienyl groups are different in the open and closed isomers.[6] In this regard, the photoreactivity of bisthienylethene in the crystalline state is of special interest because of its practical applications to optical memory. However, only limited research focused on the photochromism in the crystalline phase has been reported so far. Studies on the photochromism of metal complexes in the crystalline phase are even more sparse.[7]

Because of this, we have synthesized photochromic 1,2-bis(2′-methyl-5′-(carboxylic acid)-3′-thienyl)perfluorocyclopentene (BM-5-CATP) as a ligand, which was first reported by Branda's group in 2003.[8] Like other dicarboxylic acids such as pyridine-2,6-dicarboxylic acid[9] and biphenyl-4,4′-dicarboxylic acid,[10] BM-5-CATP may also be a versatile ligand and may function as a mono-, bi-, tri-, or tetra-dentate ligand as a result of the potential coordination abilities of the two carboxylate groups. It is expected that BM-5-CATP could connect with metal ions to form a 1D chain or 2D to 3D frameworks via various coordination fashions and subsequently result in novel applications originating from the presence of two cooperative properties in the same crystal lattice. Recently, Kojima et al. reported such a bifunctional copper complex based on a diarylethene in which the open and closed forms of the complex show obvious differences in magnetic properties.[11] Here we present the syntheses, structural characterizations, and photochromic properties of three new 1D polymers with BM-5-CATP. All of the complexes displayed reversible photochromism in the crystalline phase. Unexpectedly, $[Co(BM\text{-}5\text{-}CATP)(py)_2(MeOH)_2]$ (**1**) showed reversible chromism ascribed to MeOH-liberation/reincorporation induced by heat. The resultant desolvated form $[Co(BM\text{-}5\text{-}CATP)(py)_2]$ (**1a**) retained reversible photochromism presumably through the rearrangement of the binding of two carboxylate groups in the solid state. Furthermore, the magnetic properties of **1** have been changed upon the loss of the solvent.

Experimental Section

General Methods. Unless otherwise indicated, all of the starting materials were obtained from commercial suppliers (Aldrich, Wako, and TCI Chemicals) and were used without further purification. Infrared spectra were recorded as KBr disks on Jasco FTIR 8000 and FTIR-430 spectrometers. ^{1}H NMR spectra were measured on a JEOLGSX 270 FT NMR spectrometer at room temperature. Tetramethylsilane was used as an internal reference. Absorption spectra in the crystalline state were measured by diffuse reflectance using the Kubelka−Munk method on a Shimadzu UV-2450 spectrometer, and barium sulfate was used as a reference. Photoirradiation was carried out using a 150 W Xe lamp, and monochromatic light was obtained by passing the light through a monochromator. Direct current (dc) magnetic susceptibility data were collected on fresh microcrystalline samples restrained in eicosane to prevent torquing on a Quantum Design MPMS2 or MPMS7 SQUID magnetometer equipped with a 1 or 7 T magnet and capable of achieving temperatures of 1.7−400 K. ESR spectra were obtained on a JEOL JES-PX1050 spectrometer operating at a frequency of 9.17 GHz. Photoirradiation for the ESR spectra changes was carried out using a USHIO 500 W Xe lamp, with band-pass and cutoff filters (Toshiba V-42, O-55 and IRA-25S).

1,2-Bis(2′-methyl-5′-(carboxylic acid)-3′-thienyl) Perfluorocyclopentene (BM-5-CATP). Preparation of **b**, **c**, and **e** was based

(3) (a) Yamaguchi, T.; Uchida, K.; Irie, M. *J. Am. Chem. Soc.* **1997**, *119*, 6066−6071. (b) Yagi, K.; Soong, C. F.; Irie, M. *J. Org. Chem.* **2001**, *66*, 5419−5423. (c) Norsten, T. B.; Branda, N. R. *J. Am. Chem. Soc.* **2001**, *123*, 1784−1785. (d) Cho, H.; Kim, E. *Macromolecules* **2002**, *35*, 8684−8687. (e) Matsuda, K.; Takayama, K.; Irie, M. *Inorg. Chem.* **2004**, *43*, 482−489. (f) Jeong, Y. C.; Yang, S. I.; Ahn, K. H.; Kim, E. *Chem. Commun. (Cambridge, U.K.)* **2005**, 2503−2505.

(4) (a) Kobatake, S.; Uchida, K.; Tsuchida, E.; Irie, M. *Chem. Commun. (Cambridge, U.K.)* **2002**, 2804−2805. (b) Yamamoto, S.; Matsuda, K.; Irie, M. *Chem.—Eur. J.* **2003**, *9*, 4878−4886. (c) Kobatake, S.; Kuma, S.; Irie, M. *Bull. Chem. Soc. Jpn.* **2004**, *77*, 945−951. (d) Kobatake, S.; Shibata, K.; Uchida, K.; Irie, M. *J. Am. Chem. Soc.* **2000**, *122*, 12135−12141. (e) Kobatake, S.; Yamada, M.; Yamada, T.; Irie, M. *J. Am. Chem. Soc.* **1999**, *121*, 8450−8456.

(5) Morimoto, M.; Kobatake, S.; Irie, M. *Chem.—Eur. J.* **2003**, *9*, 621−627.

(6) Matsuda, K.; Akayama, K.; Irie, M. *Chem. Commun. (Cambridge, U.K.)* **2001**, 363−364.

(7) (a) Munakata, M.; Wu, L.-P.; Kuroda-Sowa, T.; Maekawa, M.; Suenaga, Y.; Furuichi, K. *J. Am. Chem. Soc.* **1996**, *118*, 3305−3306. (b) Fernández-Acebes, A.; Lehn, J-M. *Chem.—Eur. J.* **1999**, *5*, 3285−3292. (c) Collins, G. E.; Choi, L.-S.; Ewing, K. J.; Michelet, V.; Bowen, C. M.; Winkler, J. D. *Chem. Commun. (Cambridge, U.K.)* **1999**, 321−322. (d) Fraysse, S.; Coudret, C.; Launay, J-P. *Eur. J. Inorg. Chem.* **2000**, 1581−1590. (e) Murguly, E.; Norsten, T. B.; Branda, N. R. *Angew. Chem., Int. Ed.* **2001**, *40*, 1752−1755. (f) Konaka, H.; Wu, L.-P.; Munakata, M.; Kuroda-Sowa, T.; Maekawa, M.; Suenaga, Y. *Inorg. Chem.* **2003**, *42*, 1928−1934. (g) Matsuda, K.; Takayama, K.; Irie, M. *Inorg. Chem.* **2004**, *43*, 482−489. (h) Han, J.; Konaka, H.; Kuroda-Sowa, T.; Maekawa, M.; Suenaga, Y.; Isihara, H.; Munakata, M. *Inorg. Chim. Acta* **2006**, *359*, 99−108. (i) Han, J.; Nabei, A.; Suenaga, Y.; Maekawa, M.; Isihara, H.; Kuroda-Sowa, T.; Munakata, M. *Polyhedron* **2006**, *25*, 2483−2490. (j) Munakata, M.; Han, J.; Nabei, A.; Kuroda-Sowa, T.; Maekawa, M.; Suenaga, Y.; Gunjima, N. *Inorg. Chim. Acta* **2006**, *359*, 4281−4288. (k) Munakata, M.; Han, J.; Nabei, A.; Kuroda-Sowa, T.; Maekawa, M.; Suenaga, Y.; Gunjima, N. *Polyhedron* **2006**, *359*, 3519−3525.

(8) Myles, A. J.; Branda, N. R. *Macromolecules* **2003**, *36*, 298−303.

(9) (a) Laine, P.; Gourdon, A.; Launay, J.-P. *Inorg. Chem.* **1995**, *34*, 5129−5137. Laine, P.; Gourdon, A.; Launay, J.-P. *Inorg. Chem.* **1995**, *34*, 5138−5149. Laine, P.; Gourdon, A.; Launay, J.-P. *Inorg. Chem.* **1995**, *34*, 5156−5165. (b) Ramezanipour, F.; Aghabozorg, H.; Shokrollahi, A.; Shamsipur, M.; Stoeckli-Evans, H.; Soleimannejad, J.; Sheshmani, S. *J. Mol. Struct.* **2005**, *779*, 77−86. (c) Du, M.; Cai, H.; Zhao, X.-J. *Inorg. Chim. Acta* **2006**, *359*, 673−679. (d) Wang, L.; Wang, Z.-L.; Wang, E.-B. *J. Coord. Chem.* **2004**, *57*, 1353−1359.

(10) (a) He, X.; Lu, C.-Z.; Yuan, D.-Q.; Chen, L.-J.; Zhang, Q.-Z.; Wu, C.-D. *Eur. J. Inorg. Chem.* **2005**, *22*, 4598−4606. (b) Chun, H.; Dybtsev, D. N.; Kim, H.; Kim, K. *Chem.—Eur. J.* **2005**, *11*, 3521−3529. (c) Lee, S. W.; Kim, H. J.; Lee, Y. K.; Park, K.; Son, J. H.; Kwon, Y. U. *Inorg. Chim. Acta* **2003**, *353*, 151−158. (d) Almeida P.; Filipe A.; Klinowski, J. *Chem. Commun. (Cambridge, U.K.)* **2003**, 1484−1485. (e) Kongshaug, K. O.; Fjellvag, H. *Solid State Sci.* **2002**, *4*, 443−447. (f) Liu, G.-F.; Ye B.-H.; Ling, Y.-H.; Chen, X.-M. *Chem. Commun. (Cambridge, U.K.)* **2002**, 1442−1443. (g) Kim, J.; Chen, B.-L.; Reineke, T. M.; Li, H.-L.; Eddaoudi, M.; Moler, D. B.; O'Keeffe, M.; Yaghi, O. M. *J. Am. Chem. Soc.* **2001**, *123*, 8239−8247.

(11) Okubo, M.; Enomoto, M.; Kojima, N. *Synth. Met.* **2005**, *152*, 461−464.

Scheme 1. Synthesis of BM-5-CATP

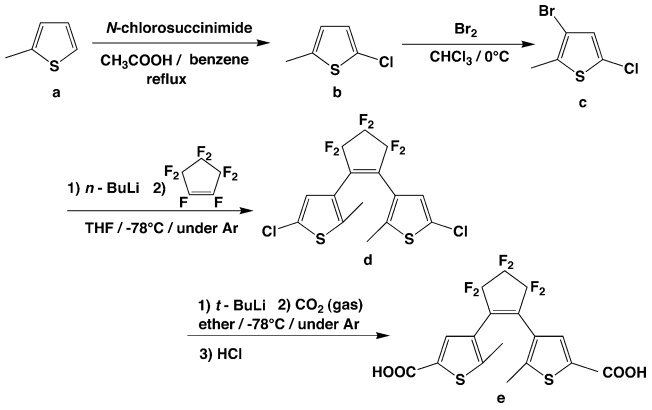

on literature methods[8,12] as shown in Scheme 1; **d** is prepared by a double substitution reaction on octafluorocyclopentene by a lithiated thiophene derivative as described below. To a stirred solution of **c** (2.0067 g, 9.49 mmol) in distilled THF (100 mL) was added dropwise an *n*-BuLi/hexane (1.65 M) solution (5.7 mL, 9.96 mmol) at −78 °C under an argon atmosphere. Stirring was continued for 20 min at the low temperature. Perfluorocyclopentene (0.6 mL) was slowly added to the reaction mixture at −78 °C, and the mixture was stirred for 2 h at that temperature. The reaction was stopped by the addition of methanol. The product was extracted with ether. The organic layer was washed with water, and then dried over $MgSO_4$, filtered, and evaporated. The crude product was purified by column chromatography on SiO_2 using hexane as the eluent, followed by recrystallization from hexane to give 0.668 g of **d** in 32.3% yield as colorless crystals. The average yield of this step is usually moderate and not easy to scale up because of the volatility of octafluorocyclopentene.[13] Single crystals of BM-5-CATP suitable for X-ray measurements were obtained by recrystallization from an EtOH solution at room temperature.

[Co(BM-5-CATP)(py)$_2$(MeOH)$_2$] (1). To a solution of BM-5-CATP (6.8 mg, 15 μmol) in pyridine (1 mL) was layered on a solution of $CoCl_2 \cdot 6H_2O$ (3.6 mg, 15 μmol) in MeOH (1 mL). Red block crystals were obtained after they were allowed to stand at room temperature for 1 month. Anal. Calcd for $C_{29}H_{26}CoF_6N_2O_6S_2$: C, 47.35; H, 3.56; N, 3.81. Found: C, 47.80; H, 3.34; N, 3.54. IR(KBr, pellet): 3079 (w), 2964 (w), 1602 (s),1579 (s), 1564 (s), 1494 (w), 1447 (s), 1433 (s), 1382(s), 1273 (s), 1186 (m), 1124 (s), 1038 (s), 985 (m), 781 (m),700 (m). UV−vis (solid state), λ_{max} 306 nm; after irradiation with 306 nm light (solid state), λ_{max} 575 nm. **1** is insoluble in common solvents, but it is soluble in pyridine.

[Co(BM-5-CATP)(py)$_2$] (1a). Light-purple **1a** was obtained as the MeOH-eliminated product of **1** after TGA (∼75 °C). Anal. Calcd for $C_{27}H_{18}CoF_6N_2O_4S_2$: C, 48.29; H, 2.70; N, 4.17. Found: C, 48.45; H, 2.51; N, 4.15. IR(KBr, pellet): 3422 (m), 1603(s), 1559 (m), 1473 (m), 1447 (m), 1386 (s), 1273 (s), 1192 (m), 1108 (s), 1039 (m), 986 (w), 775 (w). UV−vis (solid state), λ_{max} 295 nm; after irradiation with 295 nm light (solid state), λ_{max} 551 nm.

[Cu(BM-5-CATP)(py)$_3$](EtOH)(py)$_{1.8}$ (2). To a solution of BM-5-CATP (6.8 mg, 15 μmol) in pyridine (1 mL) was layered on a solution of $CuSO_4 \cdot 5H_2O$ (3.7 mg, 15 μmol) in EtOH (1 mL) in the presence of 1 drop of NEt_3. Blue platelet crystals of **2** together with small amounts of deep blue crystals [Cu(py)$_n$](SO$_4$) were obtained after 2 days. The crystals were washed with MeOH to remove the [Cu(py)$_n$](SO$_4$) complexes and dried in Ar. Anal. Calcd for the completely desolvated form of **2**, $C_{17}H_8CuF_6O_4S_2$ ([Cu(BM-5-CATP)]): C, 39.42; H, 1.56. Found: C, 39.66; H, 1.35. IR(KBr, pellet): 3462 (m), 1607 (s), 1549 (m), 1471 (m), 1450 (m), 1382(s), 1348(s), 1273 (s), 1191 (m), 1122 (m), 1071 (m), 985 (m), 774 (m). UV−vis (solid state), λ_{max} 278 nm; after irradiation with 278 nm light (solid state), λ_{max} 575 nm. **2** is insoluble in common solvents as a result of its polymeric structure.

[Zn(BM-5-CATP)(phen)(H$_2$O)] (3). BM-5-CATP (6.8 mg, 15 μmol) and 1,10-phenanthroline (hereafter referred to as phen, 2.9 mg, 15 μmol) were dissolved in 1 mL EtOH. Then, 1 mL $ZnSO_4 \cdot 7H_2O$ (4.3 mg, 15 μmol) aqueous solution was added dropwise to the above solution. The mixture was introduced into a 7 mm glass tube and sealed, which afforded **3** as colorless plate crystals after standing at ambient temperature for 1 day. Anal. Calcd for $C_{29}H_{18}ZnF_6N_2O_5S_2$: C, 48.51; H, 2.53; N, 3.90. Found: C, 48.72; H, 2.25; N, 3.71. IR(KBr, pellet): 3411(m), 3051 (w), 1587(s), 1547 (m), 1519 (m), 1494 (m), 1469(m), 1428(m), 1380 (m), 1349(m), 1273 (s), 850 (m), 726 (m). UV−vis (solid state), λ_{max} 300 nm; after irradiation with 300 nm light (solid state), λ_{max} 589 nm. **3** is insoluble in common solvents as a result of its polymeric structure.

X-ray Data Collection and Structure Solutions and Refinements. Diffraction data for the free ligand and **1**−**3** were collected on a Quantum CCD area detector coupled to a Rigaku MSC Mercury CCD diffractometer with graphite monochromated Mo Kα radiation (λ = 0.71070 Å). The intensity data were collected at 150 K (for the ligand, **1**, and **3)** and 200 K (for **2**), respectively, using the multiscan technique, and a total of 4835, 3550, 10 062, and 6448 reflections were collected for the ligand and **1**−**3**, respectively. The linear absorption coefficients μ for Mo Kα radiation is 3.29, 7.68, 6.38, and 10.88 cm^{-1}, respectively.

The structures were solved by direct methods followed by subsequent Fourier calculations.[14] The non-hydrogen atoms were refined anisotropically for all of the complexes. The final cycle of the full-matrix least-squares refinement was based on 3858, 3315, 8798, and 4258 observed reflections and 343, 290, 590, and 406 variable parameters for the ligand and **1**−**3**, respectively, converged with the unweighted and weighted agreement factors of $R = \Sigma||F_o| - |F_c|| / \Sigma |F_o|$ and $R_w = [\Sigma w(F_o^2 - F_c^2)^2/\Sigma w(F_o^2)^2]^{1/2}$. The atomic scattering factors and anomalous dispersion terms were taken from the International Tables for X-ray Crystallography, Vol. IV.[15] All of the calculations were performed using the teXsan crystallographic software package.[16]

Results and Discussion

Structural Characterizations. Details of the X-ray experiments and crystal data of the free ligand and **1**−**3** are summarized in Table 1. Selected bond lengths and bond angles are given in Table 2. Figure 1 depicts the crystal structure of the free ligand determined by X-ray crystallographic analysis. The two thienyl rings of BM-5-CATP adopt antiparallel conformations. The distance between two reactive carbons C(4) and C(10) is 3.46 Å, which is short

(12) (a) Lucas, L. N.; de Jong, J. J. D.; van Esch, J. H.; Kellogg, R. M.; Feringa, B. L. *Eur. J. Org. Chem.* **2003**, 155−166. (b) Irie, M.; Lifka, T.; Kobatake, S.; Kato, N. *J. Am. Chem. Soc.* **2000**, *122*, 4871−4876.
(13) Henne, A. L.; Latif, K. A. *J. Am. Chem. Soc.* **1954**, *76*, 610−611.
(14) Beurskens, P. T.; Admiraal, G.; Beurskens, G.; Bosman, W. P.; Gelder, R. de.; Israel, R.; Smits, J. M. M. *The DIRDIF-94 Program System*; Technical Report of the Crystallography Laboratory; University of Nijmegen, Nijmegan, The Netherlands, 1994.
(15) Cromer, D. T.; Waer. J. T. *International Tables for X-ray Crystallography*; The Kynoch Press: Birmingham, England, 1974; Vol IV.
(16) *Crystal Structure Analysis Package*; Rigaku/MSC, Inc.: Woodlands, TX, 1985 and 1992.

Table 1. Crystallographic Data for the Ligand and **1**−**3**

	L·EtOH	**1**	**2**	**3**
formula	$C_{19}H_{16}F_6O_5S_2$	$C_{29}H_{26}CoF_6N_2O_6S_2$	$C_{43}H_{38}CuF_6N_{4.8}O_5S_2$	$C_{29}H_{18}ZnF_6N_2O_5S_2$
fw	502.44	735.58	943.66	717.96
cryst. syst.	monoclinic	orthorhombic	orthorhombic	monoclinic
space group	$P2_1/c$(No.14)	*Pnna*/(No.52)	*Pna*21/(No.33)	$P2_1/n$(No.14)
a/Å	10.971(5)	15.695(6)	16.0646(9)	15.47(1)
b/Å	17.243(7)	22.081(8)	24.026(2)	11.611(8)
c/Å	11.768(5)	8.969(3)	11.9054(7)	17.05(1)
β/°	105.971(5)			110.892(7)
V/Å^3	2285(1)	3108(4)	4595.2(5)	2861(3)
Z	4	4	4	4
D/g·cm^{-3}	1.559	1.572	1.364	1.667
μ/cm^{-1}	3.29	7.68	6.38	10.88
T/K	150	150	200	150
obsd reflns ($I > 2\sigma(I)$)	3858	3315	8798	4258
R[a]	0.0774	0.0538	0.0639	0.1122
R_w[b]	0.2077	0.0980	0.1265	0.2021
GOF	1.171	1.303	1.119	1.162

[a] $R = \Sigma||F_o| - |F_c||/\Sigma|F_o|$. [b] $R_w = [\Sigma w(F_o^2 - F_c^2)^2/\Sigma w(F_o^2)^2]^{1/2}$.

Table 2. Selected Bond Length (Å) and Angles (deg) for **1**−**3**[a]

		1	
Co(1)−O(1/1*)	2.075(2)	Co(1)−O(3/3*)	2.135(2)
Co(1)−N(1)	2.128(3)	Co(1)−N(2)	2.153(3)
O(1)−Co(1)−O(3)	87.53(7)	O(1*)−Co(1)−O(3)	92.35(7)
O(1)−Co(1)−O(3*)	92.35(7)	O(1*)−Co(1)−O(3A*)	87.53(7)
N(1)−Co(1)−N(2)	180.0		
		2	
Cu(1)−O(1)	1.949(3)	Cu(1)-O(3#)	1.953(3)
Cu(1)−N(1)	2.296(4)	Cu(1)−N(2)	2.037(3)
Cu(1)−N(3)	2.042(4)		
N(1)−Cu(1)−N(2)	97.0(1)	N(1)−Cu(1)−N(3)	101.5(1)
N(2)−Cu(1)−N(3)	161.5(1)	O(1)−Cu(1)−O(3#)	177.5(1)
		3	
Zn(1)−N(1)	2.100(6)	Zn(1)−N(2)	2.108(6)
Zn(1)−O(1)	2.023(5)	Zn(1)−O(3A)	2.004(6)
Zn(1)−O(5)	2.087(5)		
N(1)−Zn(1)−N(2)	79.2(2)		
O(1)−Zn(1)−O(5)	80.8(2)	N(2)−Zn(1)−O(5)	90.9(2)
N(2)−Zn(1)−N(1)	79.2(2)	N(1)−Zn(1)−O(1)	86.1(2)

[a] Symmetry code, **1**: (*) x, $^1/_2 - y$, 1.5 − z; (A) $^1/_2 - x$, −y, −z; **2**: (#) $^1/_2 + x$, $^1/_2 - y$, $-1 + z$; **3**: (A) $^1/_2 + x$, 1.5 − y, $-^1/_2 + z$.

enough for the occurrence of a cyclization/cycloreversion in the crystalline phase.[4a] F atoms are disordered.

In the three metal complexes, BM-5-CATP acts as a bis-monodentate bridging ligand through one of the oxygen atoms of each carboxylate group to generate the 1D polymers. **1** is revealed as a zigzag chain with the neighboring ligands in a syn-anti fashion by X-ray single-crystal diffraction as shown in Figure 2. In one unit, each cobalt is coordinated to two O atoms from two ligands (Co(1)−O(1/1*) = 2.075(2) Å), two N atoms from pyridine (Co(1)−N(1) = 2.128(3) Å, Co(1)−N(2) = 2.153(3) Å), and two methanol molecules (Co(1)−O(3/3*) = 2.135(2) Å), forming a slightly distorted octahedron structure. Two carboxylate oxygens from the ligand (O(1) and O(1*)) and two oxygens from the methanol (O(3) and O(3*)) comprise the equatorial plane, whereas the axial positions are filled by the other two nitrogen atoms from pyridine (N(1)−Co(1)−N(2) = 180.0°). The bond lengths of Co−N and

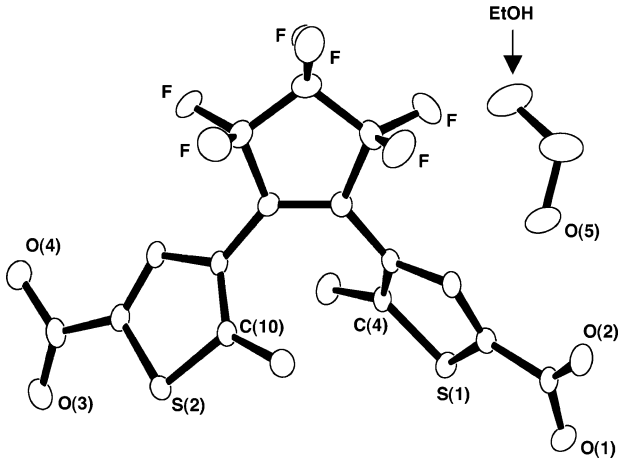

Figure 1. ORTEP view with an atomic labeling scheme of BM-5-CATP, showing 50% thermal ellipsoids.

Co−O (ligand) are well within the range of the (Co−pyridine and carboxylate) complexes.[17] Other bond lengths and angles are unexceptional.

In the asymmetric unit of **2**, the Cu is five-coordinated to three N atoms from pyridine and two O atoms from ligands. The five-coordinated system was evaluated by the geometric τ parameter ($\tau = (\beta - \alpha)/60$).[18] The τ value is 0.27 in **2**, indicating that it may be best described as having distorted square-pyramidal geometry. Note that two O atoms (O(1) and O(3#)) and two N atoms (N(2) and N(3)) are bonded to the Cu center at the corners of the square (Cu(1)−O(1) = 1.949(3) Å, Cu(1)−O(3#) = 1.953(3) Å, Cu(1)−N(2) = 2.037(3) Å, Cu(1)−N(3) = 2.042(4) Å). The apical position is occupied by another N atom with a longer bond (Cu(1)−

(17) (a) Groeneman, R. H.; Macgillivray, L. R.; Atwood, J. L. *Inorg. Chem.* **1999**, *38*, 208−209. (b) Pan. L.; Ching, N.; Huang, X.-Y.; Li, J. *Inorg. Chem.* **2000**, *39*, 5333−5340. (c) Maspoch, D.; Ruiz-Molina, D.; Wurst, K.; Rovira, C.; Veciana, J. *Polyhedron* **2003**, *22*, 1929−1934. (d) March, R.; Clegg, W.; Coxall, R. A.; Cucurull-Sánchez, L.; Lezama, L.; Rojo, T.; González-Duarte, P. *Inorg. Chim. Acta* **2003**, *353*, 129−138.

(18) (a) Addison, A. W.; Rao, T. N. *J. Chem. Soc., Dalton Trans.* **1984**,-1349−1356. (b) Murphy, G.; Nagle, P.; Murphy, B.; Hathaway, B. *J. Chem. Soc., Dalton Trans.* **1997**, 2645−2652. (c) Brophy, M.; Murphy, G.; O'sullivan, C.; Hathaway, B.; Murphy, B. *Polyhedron* **1999**, *18*, 611−612. (d) Maekawa, M.; Konaka, H.; Sugimoto, K.; Suenaga, Y.; Kuroda-Sowa, T.; Munakata, M. *Anal. Sci.* **2004**, 71−72.

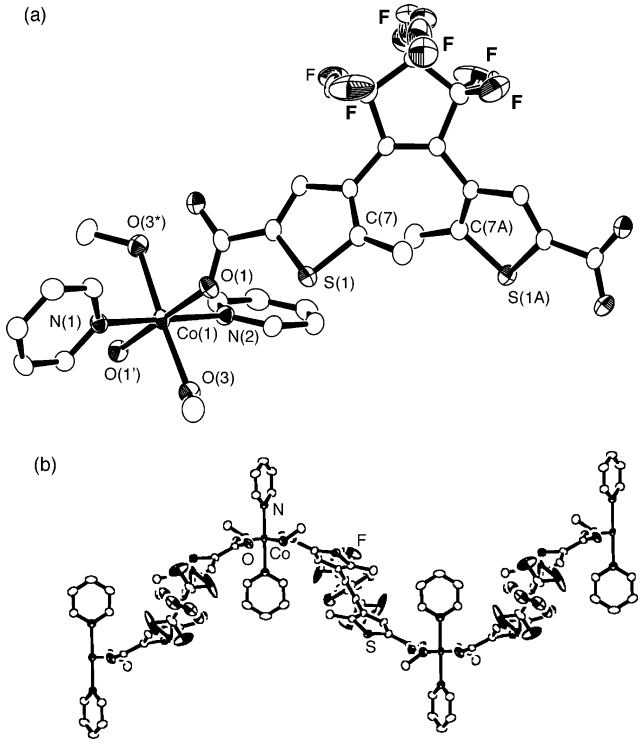

Figure 2. Crystal structure of **1**. (a) ORTEP view with atomic labeling scheme showing 50% thermal ellipsoids and (b) 1D chain. Symmetry code: *, x, $^1/_2 - y$, $1.5 - z$, A, $^1/_2 - x$, $-y$, $-z$.

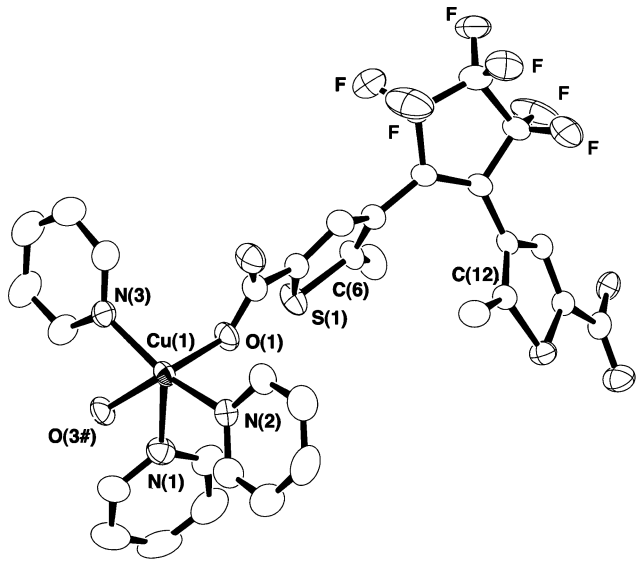

Figure 3. Crystal structure of **2**. ORTEP view with atomic labeling scheme showing 50% thermal ellipsoids. Solvent molecules were omitted for clarity. Symmetry code: #, $^1/_2 + x$, $^1/_2 - y$, $-1 + z$.

N(1) = 2.296(4) Å) (Figure 3). Both the Cu−O and Cu−N distances fall within the expected values.[19] Similar to **1**, in **2** the ligands were also attached to the metal center in trans conformations, forming a syn-anti polymeric structure.

The local coordination environment of **3** can be described as a distorted square-pyramidal structure with an index τ parameter of 0.35 (Figure 4a). Each phen acts as a terminal ligand with typical Zn−N distances of Zn(1)−N(1) = 2.100(6) and Zn(1)−N(2) = 2.108(6) Å and a chelating angle of N(1)−Zn(1)−N(2) = 79.2(2)°.[20] The remaining coordination positions of the metal atom are saturated by the bis-monodentate BM-5-CATP (Zn(1)−O(1) = 2.023(5), Zn(1)−O(3A) = 2.004(6)) and one water molecule (Zn(1)−O(5) = 2.087(5)). Two N atoms and two O atoms (O(1) and O(5)) are in equatorial positions, and O(3A) is in the apical position. There are intramolecular O−H···O hydrogen bonds between coordinated H_2O and adjacent carboxyl O atoms that further stabilize the coordination structures. The ligands in **3** were bonded to Zn ions in a cis conformation, which differs from the trans conformations of the ligands in **1** and **2**, as a result of the bulky phen. Thus, **3** shows a syn−syn chain structure (Figure 4b).

The two thienyl rings in **1**−**3** adopt antiparallel configurations. In **2** and **3**, the distances of 3.53 and 3.57 Å between two reactive carbons (C(6)−C(12)) are slightly longer than that of metal-free (BM-5-CATP 3.46 Å), whereas the reactive distance of 3.39 Å (C(7)−C(7A)) in **1** is shorter than that of BM-5-CATP. All of the distances are less than 4 Å and thus are close enough to undergo the photocyclization, indicating the possible photoreactivities in the solid state.[4a]

The assembly processes of the frameworks of metal complexes are highly influenced by many factors such as metal ions, counter anions, solvents, temperature, pH value, and the ratio of metal to ligand. In this study, only one coordination mode was observed although, theoretically, dicarboxylate could have versatile coordination methods. It is expected that various coordination features could be obtained in a later program by rationally selecting the counter anions of the metal salts and the co-ligand.

Photochromism of BM-5-CATP. The photochromic reaction of the free ligand (BM-5-CATP) was examined in the solid state (Figure 5). Before irradiation, colorless powders of BM-5-CATP have intense absorption bands at ca. 305 nm, which are ascribed to the intraligand $\pi \rightarrow \pi^*$ and n $\rightarrow \pi^*$ transitions of the thiophene rings. Upon UV irradiation of the ligand at 305 nm, a strong peak at 610 nm and a moderate peak at ca. 390 nm emerged in the absorption spectrum. It is indicated that the open form was transferred to the closed form, and the photoinduced purple color originates from the closed form. Upon excitation into the absorption bands of the closed form (610 nm), absorptions due to the closed form decreased in intensity, indicative of the regeneration of the open form as a result of photocycloreversion. Thus, reversible photochromism occurred in BM-5-CATP in the solid phase (Scheme 2). The maximum absorption of the closed isomer of BM-5-CATP is at a much longer wavelength than those of BM-2-PTP (bis(2′-methyl-5′-(2″-pyridyl)-3′-thienyl)perfluorocyclopentene) and *cis*-dbe (*cis*-1,2-dicyano-1,2-bis(2,4,5-trimethyl-3-thienyl)ethene),

(19) (a) Balogh-Hergovich É.; Kaizer, J.; Speier, G.; Argay, G.; Párkányi, L. *J. Chem. Soc., Dalton Trans.* **1999**, 3847−3854. (b) Speier, G.; Selmeczi, K.; Pintér, Z.; Huttner, G.; Zsolnai, L. *Z. Kristallogr.* **1998**, *213*, 263−264. (c) Ghosh, S. K.; Bharadwaj, P. K. *Inorg. Chem.* **2004**, *43*, 6887−6889. (d) Cui, Y.; Ngo, H.-L.; Lin, W. *Inorg. Chem.* **2002**, *41*, 1033−1035.

(20) (a) Baggio, R.; Garland, M. T.; Perec, M. *J. Chem. Soc., Dalton Trans.* **1996**, 2747−2753. (b) Sun, D.-F.; Cao, R.; Liang, Y.-C.; Shi, Q.; Su, W.-P.; Hong, M.-C. *J. Chem. Soc., Dalton Trans.* **2001**, 2335−2340. (c) Wei, D.-Y.; Zheng, Y.-Q.; Lin, J.-L. *Z. Anorg. Allg. Chem.* **2002**, *628*, 2005−2012.

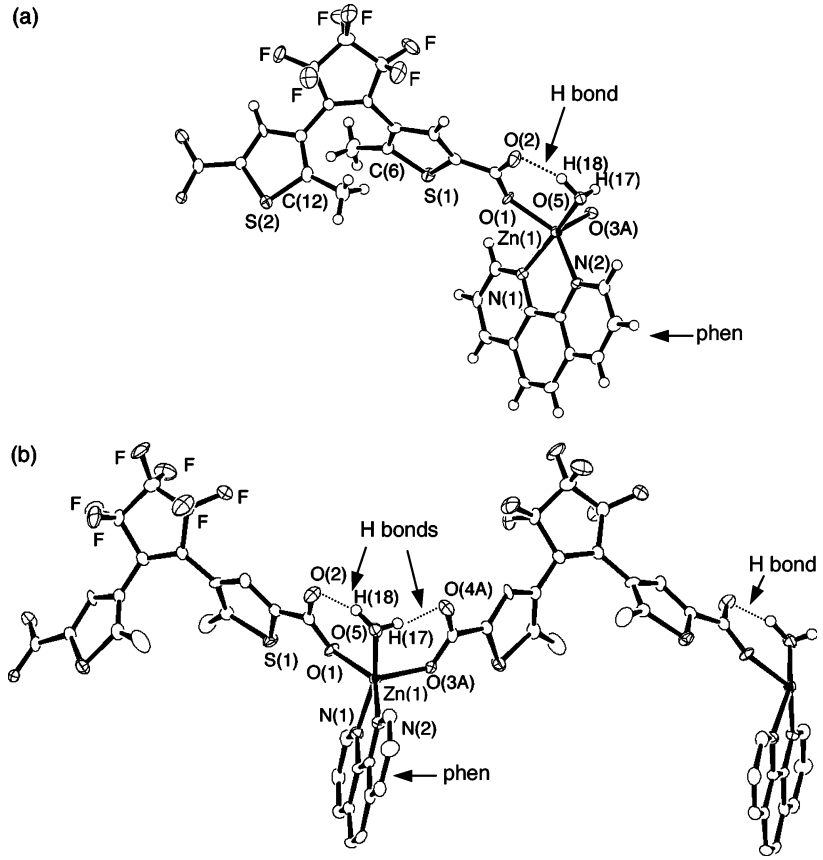

Figure 4. Crystal structure of **3**. (a) ORTEP view with atomic labeling scheme, showing 50% thermal ellipsoids; the H bonds are indicated as dotted lines and (b) 1D chain, showing only the H atoms involved in H bonds. Symmetry code: A, $^1/_2 + x$, $1.5 - y$, $-^1/_2 + z$.

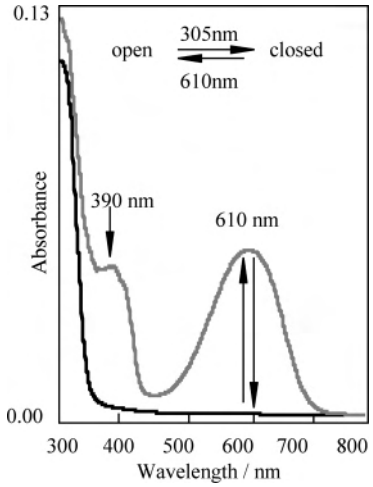

Figure 5. Absorption spectral changes of BM-5-CATP in the solid state.

Scheme 2. Photochromic Reaction of BM-5-CATP in the Solid State

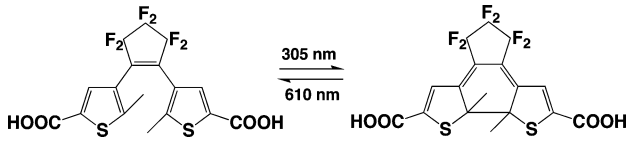

which were observed at 580 and 520 nm in the solid state, respectively.[7i,j]

IR Spectra. The IR analyses provide useful information and showed that the characteristic COOH peak of 1688 cm^{-1} in BM-5-CATP is absent in **1**−**3**, indicating the carboxylate groups are deprotonated. The ν_s(O−H) around 3411 cm^{-1} indicates the presence of a coordinated H_2O molecule in **3**. The typical $\nu_{as}(CO_2)$ and $\nu_s(CO_2)$ bands are observed at 1579, 1564, 1382, and 1360 cm^{-1} for **1**, at 1549 and 1348 cm^{-1} for **2**, and at 1587 and 1380 cm^{-1} for **3**, respectively. However, the $\nu_{as}(CO_2)$ band is shifted to 1559 and 1542 cm^{-1} in **1a** with the $\nu_s(CO_2)$ band observed at 1386 and 1348 cm^{-1}. The Δ values ($\Delta = \nu_{as}(CO_2) - \nu_s(CO_2)$) in the range of 197−207 cm^{-1} indicated the presence of uncoordinated oxygen atoms of the ligand in **1**−**3**, consistent with the X-ray analysis results.[21] The comparatively low Δ value (173 cm^{-1}) of **1a** presumably suggests that the binding mode of the carboxylate is transformed to chelating−bridging (or bis-bidentate) after the loss of the solvent.

Thermogravimetric Analysis and Photochromism of 1 and 1a. Thermal gravimetric analysis (TGA) of **1** revealed the first-step weight loss of 9.2% (calcd 9.1%) from 60 to 75 °C, corresponding to the release of two coordinated MeOH molecules per formula unit with a color change from red to light purple, which originates from the loss of the solvent (Figure S1). A ^{1}H NMR resonance of MeOH (3.63 ppm) was observed in the pyridine-d_5 of **1** (before heating, Figure 6a), but it disappeared in **1a** (after heating at 75 °C, Figure 6b). The crystalline powder of **1a** immersed in MeOH regenerated the original red product. A signal at 3.63 ppm

(21) (a) Deacon, B. G.; Philips, R. J. *Coord. Chem. Rev.* **1980**, *33*, 227−250. (b) Massoud, S. S.; Mautner, F. A.; Vicente, R.; Sweeney, H. N. *Inorg. Chim. Acta.* **2006**, *359*, 1489−1500. (c) Chen, B.-L.; Mok, K.-F.; Ng, S.-C.; Drew, M. G. B. *Polyhedron*, 1999, *18*, 1211−1220. (d) Fan, S.-R.; Zhu, L.-G. *Inorg. Chem.* **2006**, *45*, 7935−7942.

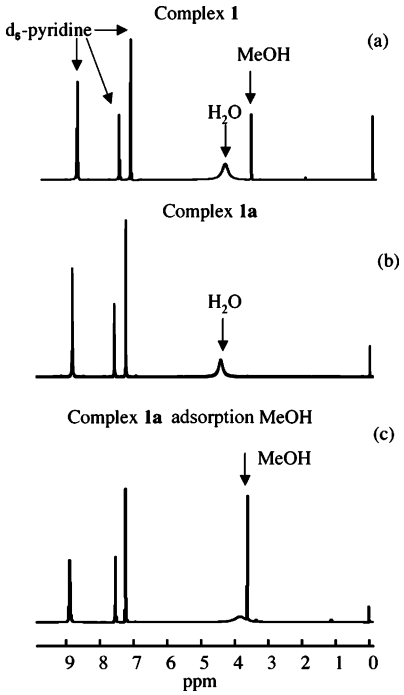

Figure 6. ^{1}H NMR spectra of (a) **1**, (b) **1a**, (c) MeOH absorption of **1a** in pyridine-d_5 at room temperature.

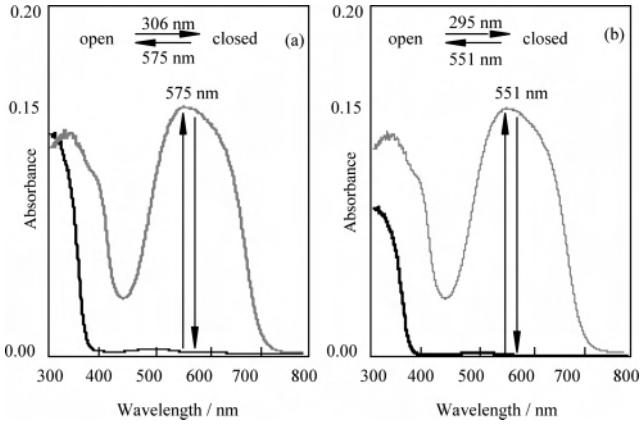

Figure 7. Absorption spectral changes of (a) **1** and (b) **1a** in the crystalline phase.

in the ^{1}H NMR spectrum was observed again, indicating that methanols are incorporated into **1** (Figure 6c). This result shows that reversible chromism via MeOH liberation/adsorption occurred in **1**. It is noted that **1** changes color upon heating, but this chromism is not attributable to the transformation from open form to closed form induced by heat (thermochromism) because the UV spectra of **1a** did not show characteristic peaks of the closed-ring form in the visible bands.

Subsequently, photochromism was examined for both **1** and **1a** in the crystalline phase, respectively (Figure 7). Before irradiation, **1** and **1a** have absorptions at 306 and 295 nm in the UV region, respectively. Irradiation with 306 and 295 nm light leads to peaks at 575 and 551 nm for **1** and **1a**, respectively, with color changes from red and light purple to deep purple, respectively. The deep-purple color originated from the closed-ring form. After further excitation with 575 and 551 nm light on the closed forms of **1** and **1a**, the

Scheme 3. Photochromism of Complexes **1** and **1a** in the Crystalline Phase

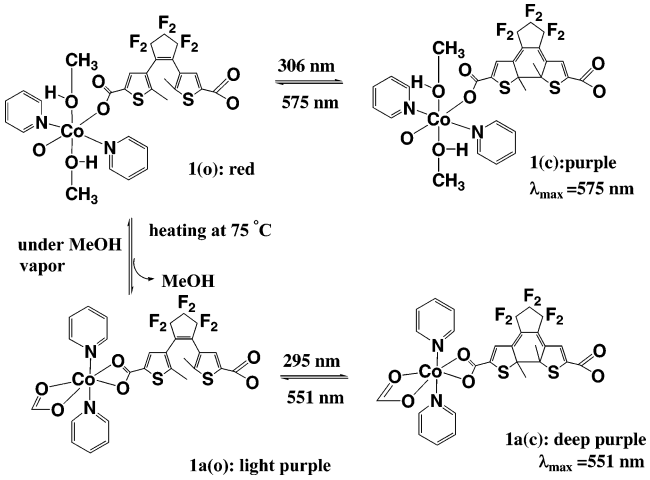

absorptions in the visible region gradually flattened, and the accompanying deep-purple color changed back to the initial color. The λ_{max} of **1a** (551 nm) in closed form shifted to a shorter wavelength compared with that of **1** (575 nm). Thus, the most remarkable features of **1** are its ability to display reversible photochromism before and after the removal of the coordinated solvent in the crystalline state and reversible chromism as a result of MeOH liberation/reincorporation (Scheme 3).

As the IR analyses indicated, **1** displayed a rare color and structural changes, presumably via changes in the coordination modes in the solid state induced by the removal of solvent.[22] Even less common are the retention of photochromism and the changes in magnetic properties. (The magnetic properties are described below.) Upon heating, a single-crystal to single-crystal transformation fails to occur in **1**, and thus, exact structural information of its desolvated form is unavailable. However, its retention of photochromism suggested that the framework of the ligand in **1** did not decompose after the liberation of the MeOH. The maximum absorption of **1a** (551 nm), which is significantly different from that of the free ligand (610 nm), further indicated that the rearranged coordination framework was not destroyed.

Photochromism of 2 and 3. As described in the structure characterization, the two thienyl rings in **2** and **3** adopt antiparallel arrangements, and the distances between the reactive carbons are short enough for photocyclization. These essential conditions are favorable for a photochromic reaction in the crystalline state to occur. Figure 8a,b shows the absorption spectral changes of **2** and **3**, respectively. The open forms of **2** and **3** have shoulders at ca. 278 nm and 300 nm, respectively, which are agreeable with the shoulder of free BM-5-CATP (305 nm). Upon irradiation with 278

(22) (a) Jia, J.-H.; Lin, X.; Blake, A. J.; Champness, N. R.; Hubberstey, P.; Shao, L. M.; Walker, G.; Wilson, C.; Schrolder M. *Inorg. Chem.* **2006**, *45*, 8838−8840. (b) Dinca, M.; Long, J. R. *J. Am. Chem. Soc.* **2005**, *127*, 9376−9377. (c) Takaoka, K.; Kawano, M.; Tominaga, M.; Fujita, M. *Angew. Chem., Int. Ed.* **2005**, *44*, 2151−2154. (d) Chen, C.-L.; Goforth, A. M.; Smith, M. D.; Su, C.-Y.; zur Loye, H.-C. *Angew. Chem., Int. Ed.* **2005**, *44*, 6673−6677. (e) Biradha, K.; Fujita, M. *Angew. Chem., Int. Ed* **2002**, *41*, 3392−3395. (f) Suh, M. P.; Ko, J. W.; Choi, H. J. *J. Am. Chem. Soc.* **2002**, *124*, 10976−10977.

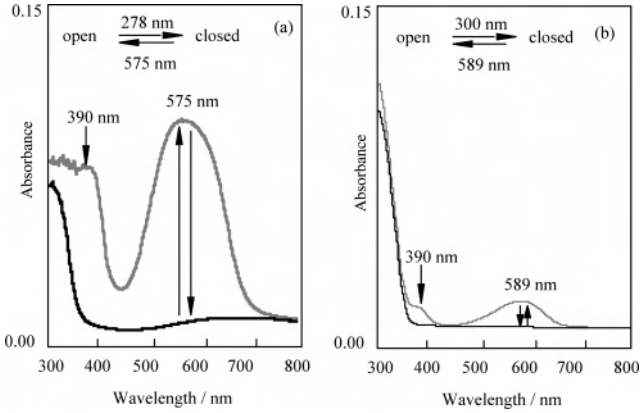

Figure 8. Absorption spectral changes of (a) **2** and (b) **3** in the crystalline phase.

and 300 nm light, the blue and colorless crystals turned purple, and new absorptions at 575 and 589 nm were observed for **2** and **3**, respectively, indicative of the formation of the closed-form conformers. The purple species reverted to their initial color by further irradiation with 575 and 589 nm light, respectively, showing the reversible photochromic properties in the crystalline phase. Compared with that of the free BM-5-CATP (λ_{max} = 610 nm), both of the λ_{max} values of the closed forms of **2** and **3** shifted to a shorter wavelength as a result of an increase in the strain upon complexation. There are no remarkable changes in the absorbance of **3**, suggesting that the transformation ratio from the open to closed form is lower and photochromism occurred only on the surface of the crystals. This is partially due to the steric hindrance of the bulky phen during the rotation of two thienyl rings along the C−C bond between the thiophene and ethylene moieties. Also, there are intramolecular H bonds, which allow**3** to pack more closely than **1** and **2**. Therefore, the photocyclizations might be suppressed by the rigidity of the close packing. Although **3** is not suitable for practical application, more work has to be done to understand the real factors that affect the photochromic properties of the complexes. Theses factors may include the coordination polyhedron around the metal center, the role of intramolecular and intermolecular H bonds, and the packing structures.

Magnetic Properties. Solid-state, variable-temperature magnetic susceptibility measurements for **1** and **1a** were performed along with photochromism. dc magnetic susceptibility (χ_M) data were collected from 2 to 280 K under a 1.0 T magnetic field (Figure S2). For **1** and **1a**, the behaviors are similar to each other. The room-temperature $\chi_M T$ values of 3.55 and 2.89 $cm^3 \cdot K \cdot mol^{-1}$ for **1**(o) and **1a**(o) (where o = open form), respectively, are larger than the spin-only value of 1.875 $cm^3 \cdot K \cdot mol^{-1}$ for an uncoupled high-spin octahedral Co(II) ion ($S = {}^3/_2$, $g = 2$), in accordance with the well-documented orbital contribution of the octahedral Co(II).[23] Compared with **1**, the room-temperature $\chi_M T$ value

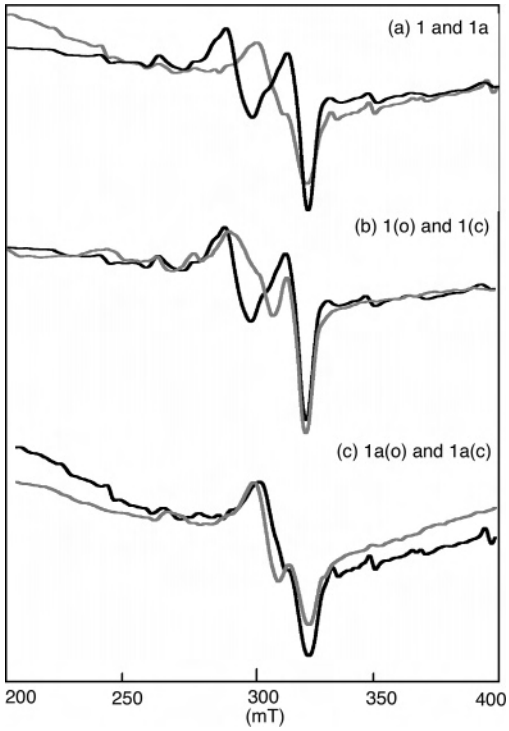

Figure 9. X-band ESR spectra of (a) **1** (black) and **1a** (gray); (b) **1**(o) (black) and **1**(c) (gray); and (c) **1a**(o) (black) and **1a**(c) (gray).

of complex **1a**(o) is smaller. X-band ESR spectra of **1** and **1a** also showed obvious differences (Figure 9). These results showed that the changes in metal coordination structures induced by heat can lead to changes not only in color but also in magnetic properties, which may give rise to potential applications as multifunctional materials.

Similar magnetic susceptibility spectral shapes were observed for **1**(c) and **1a**(c) (where c = closed form), but no marked changes in $\chi_M T$ values were observed in comparison to those of the open-form isomers. This indicated that the cobalt−cobalt interactions through the long bridging BM-5-CATP are weak so that the differences in magnetic susceptibility cannot be detected between the open form and closed form. The ESR spectral changes were observed in all cases. The differences of **1**(o) with **1**(c) and **1a**(o) with **1a**(c) suggested that the stretching shrinkages of the BM-5-CATP accumulated in the polymer structure along with photocyclization.[13] For **2**(o) and **2**(c), no obvious changes were observed (Figure S3).

Conclusions

We have prepared photochromic BM-5-CATP and its three transition-metal complexes successfully, and all of the structures have been characterized by X-ray diffraction analysis. The main findings are summarized as follows: (1) Polymers **1** and **2** displayed typical photochromic reactions in the crystalline phase. The complexation of metal ions did not suppress the photochromism in the crystalline state. (2) In particular, **1** underwent a solid-state structural transformation via the liberation of bound MeOH upon heating. More surprisingly, the dynamic structural changes did not prohibit the reversible photoisomerization of the generated MeOH-

(23) (a) Liu, F.-C.; Zeng, Y.-F.; Jiao, J.; Bu, X.-H.; Ribas, J.; Batten, S. R. *Inorg. Chem.* **2006**, *45*, 2776−2778. (b) Kapoor, R.; Kataria, A.; Venugopalan, P.; Kapoor, P.; Hundal, G.; Corbella, M. *Eur. J. Inorg. Chem.* **2005**, *19*, 3884−3893. (c) Rodríguez, A.; Kivekäes, R.; Colacio, E. *Chem. Commun. (Cambridge, U.K.)* **2005**, 5228−5230.

desolvated form (**1a**), indicating retention of the framework and excellent stability. (3) In addition to the color change, the SQUID and ESR spectra show obvious changes initiated by the removal of MeOH. The behaviors of **1** indicate the potential multifunctions of photochromic complexes originating from the coordination framework and the photochromic ligand. (4) The results of this work show that the coordination geometry and packing of the compounds significantly affect the photochromic performance. These findings suggest a series of follow-up experiments to understand further the relationship between the coordination structures and the photochromic properties triggered by light. Clearly, by rational design of metal ions, co-ligands, and counter anions, photochromic behaviors could be controlled or modified.

Acknowledgment. This work was partially supported by Grants-in-Aid for Science Research (nos. 14340211 and 16350037) from the Ministry of Education, Science, Sports and Culture in Japan.

Supporting Information Available: TGA analysis of **1**, magnetic properties of **1** and **1a**, and X-ray crystallographic data for BM-5-CATP and **1**−**3** in CIF format. This material is available free of charge via the Internet at http://pubs.acs.org.

IC0615168